# Electromagnetic Scattering of THz Waves from a Microsize Graphene-Sandwiched Thin Dielectric Strip

Taner Oğuzer
Department of Electrical and Electronics Engineering
Dokuz Eylul University, Buca, 35160 Izmir, Turkey
taner.oguzer@deu.edu.tr

Ayhan Altintas
Department of Electrical and Electronics Engineering
Bilkent University, 06800 Ankara, Turkey
altintas@ee.bilkent.edu.tr

***Abstract*— Two-dimensional (2-D) scattering of the H-polarized plane wave by a composite flat material strip is investigated. It is made as graphene-dielectric-graphene sandwich-like structure which is placed in the free space. Our modeling uses singular integral equations and Nystrom discretization. The total scattering cross-section and the absorption cross-section are computed, together with the relative error plots for the current and the far field. The surface plasmon resonances on the graphene strips and the thin dielectric layer performance are evaluated.**

***Keywords—electromagnetic scattering;strip; resonance.***

## I. INTRODUCTION

Graphene is an innovative atomically-thin material [1] offering the numerous applications from the infrared range for nanosize samples to the THz range for the microsize ones. One of the main properties is its frequency dependent conductivity, with can be used to design various tunable components. Besides, it can support the Surface Plasmon (SP) lossy guided wave. This wave produces Fabry-Perot type resonances due to reflections from the edges of patterned graphene. Graphene has also the applications in the infrared nanosensor systems and can be used in optical elements [2].

An important property of the graphene is that its electrical conductivity can be adjusted and controlled by applying an external electrostatic biasing field. This d-c biasing changes the graphene chemical potential and it can be applied to the graphene sample using a supporting dielectric substrate. In the basic simulations, it is often assumed that the graphene strip is located in the free space and its biasing still exists in some way. In the graphene strips, the edge effects become important if the strip width gets smaller than 100 nm. For wider strips one can disregard these edge effects and use the electron conductivity model developed for infinite graphene layer. In the THz range, which is actively explored in today's electromagnetic-wave technology, various graphene-based devices, circuits and systems are anticipated, designed and developed [1].

Assuming a graphene strip has zero thickness, the simulations can be performed by using the electromagnetic boundary value problem (BVP) whose formulation involves the resistive-sheet boundary condition [3,4]. However in the present study, we intend to model a more realistic graphene strip configuration with a substrate material sheet. To do this, we follow the generalized boundary conditions (GBC) [5] and its improved version [6] for the case of the composite graphene-dielectric-graphene model [7].

In the full-wave modeling of the scattering from the strips, finite-difference time-domain method is the one of the widespread techniques. However it needs large number of unknowns for the discretization of the physical domain around the object. It also has a disadvantage in the poor satisfaction of the far field radiation condition. The method of moments (MoM) technique can also be applied to the strip geometries. Still if used with local basis functions, its accuracy fails to exceed the level of 2-3 digits in the surface current even on a-few-wavelengths-wide strips.

The method of analytical regularization MAR [8] can be thought as a perfect alternative. In MAR, the kernel of the singular integral equations (SIE) is separated into two parts, the more singular part and the remainder. Then the more singular part is analytically inverted using some specialized functional techniques like the Riemann-Hilbert Problem (RHP) method. The remainder leads to the Fredholm second-kind matrix equation that provides a convergent numerical solution. The SIE-MAR technique enables one to perform the accurate full wave analysis of the perfectly-conducting and imperfect reflector antenna characteristics [9,10] and the scattering performances of the other strip geometries including graphene [11-13].

Another convergent method, which can be used especially for simple geometries with a high accuracy, is the Nystrom method [14]. It has been used in the modeling of the wave scattering from the strips and it produces a rapid and economic solution. This makes it very attractive alternative. The main property is the guaranteed convergence with the easily controlled accuracy of computations. When we look to the literature we can see the various accurate simulations of the strip type geometries with Nystrom method. For example the thin strips of dielectric material were modeled in [15]. The

978-1-5386-5438-5/18/$31.00 ©2018 IEEE

finite graphene strip grating was reduced to SIE and its Nystrom solution was performed in [16,17]. In the recent work [18], the bulk refractive index sensitivities of resonances on a microsize graphene strip were studied.

In the present study, we combine a thin dielectric strip and two graphene layers together as a composite graphene-dielectric-graphene model. We use the thin layer GBC and so the inner field inside the thin composite is neglected. It is viewed as an infinitely thin strip and only the fields just above and below the structure are used. Then the corrected resistivity coefficients obtained for the graphene-sandwiched model are applied to the numerical modeling of the scattering from this composite strip using the GBC. To simulate the graphene, previously known expressions of its surface conductivity are used as a Kubo formula [19]. Then two decoupled SIEs are obtained from the electromagnetic BVP formulation and these are solved by the Gauss-Legendre and Chebyshev quadrature formulas, valid for the singular and hyper singular kernels. This type of solution provides us accurate data in the determination of the scattering and absorption characteristics. The total scattering and absorption cross sections of this combined strip that enables us to identify and analyze the SP-mode resonances at the lower THz frequencies. This analysis meets no difficulties if extended to the higher frequency range.

## II. Formulation

The problem geometry with the illumination by an H-polarized electromagnetic plane wave is presented in Fig. 1. The incident angle $\varphi_{in}$ is measured from the $x$-axis. The strip has the thickness $h$ << $\lambda_0$. Two grapheme layers cover this thin material strip from both sides. We assume that the inner material of the strip is dielectric with relative permittivity $\varepsilon_r$ and the unity relative permeability ($\mu_r = 1$).

The rigorous formulation of the considered BVP can be stated in terms of the Helmholtz equation, the Sommerfeld radiation condition far from the strip [20]. The thin layer GBC is used with its composite sandwiched model [6]. It was applied to a thin layer dielectric disk sandwiched between two graphene disks and excited by a short dipole in [7].

We apply the same boundary condition for the considered strip geometry. In this GBC model, the inner field is again not considered and strip is viewed as infinitely thin. However the effect of the graphene layers and the inner thin dielectric can be seen in the modified resistivities. This modified condition can be written as the following pair of equations:

$$[\vec{E}^{+}_{\tan}+\vec{E}^{-}_{\tan}]/2 = Z_0\, R_{GDG}\, \underbrace{\vec{n}\times[\vec{H}^{+}_{z}-\vec{H}^{-}_{z}]}_{\hat{z}V_z}, \tag{1a}$$

$$[\vec{H}^{+}_{z}+\vec{H}^{-}_{z}]/2 = Q_{GDG}/Z_0\, \underbrace{-\vec{n}\times\left[\vec{E}^{+}-\vec{E}^{-}\right]}_{\hat{x}W_x}, \tag{1b}$$

where $V_z$ and $W_x$ are the equivalent magnetic and electric type surface currents, $\vec{n}$ is the unit normal vector to the surface of the layer, directed from the lower half-space to the upper half-space, $Z_0$ is the impedance of the free space. Parameters $R_{GDG}$ and $Q_{GDG}$ are called the relative electric and magnetic resistivities of the overall graphene covered strip geometry.

Following [6,7], we obtain these modified electric and magnetic resistivities as follows:

$$R_{GDG} = \frac{R}{1+2Z_0\, R\,\sigma}, \tag{2a}$$

$$Q_{GDG} = \frac{1}{2} Z_0\,\sigma + Q, \tag{2b}$$

where the electric and magnetic resistivities of a stand-alone single and high-contrast ($|\varepsilon_r| >> 1$) thin dielectric layer are

$$R = \frac{i}{2}\sqrt{\frac{1}{\varepsilon_r}}\cot\left(\sqrt{\varepsilon_r}\,\frac{k_0 h}{2}\right) \tag{3a}$$

$$Q = \frac{i}{2}\sqrt{\varepsilon_r}\cot\left(\sqrt{\varepsilon_r}\,\frac{k_0 h}{2}\right) \tag{3b}$$

Here the $k_0$ is the free space wavenumber and the relative dielectric permittivity $\varepsilon_r$ can be either real or complex. If the relative permittivity takes a complex value with a positive imaginary part, such boundary conditions simulate a lossy dielectric layer. Note that in the case of a symmetrically sandwiched layer the cross-resistivity equals to zero (see [5[).

In (2), σ is the graphene surface conductivity; it is given in [19] with the aid of Kubo formalism, as a sum of intraband and interband contributions.

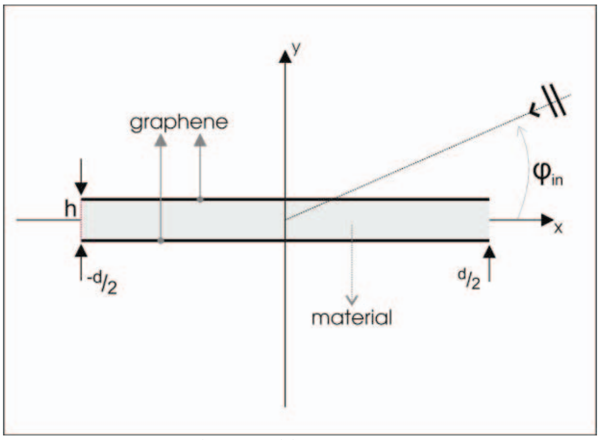


Fig. 1: Problem Geometry

The scattered field components can be written as integrals,

$$H_z^{sc} = -(k_0/4Z_0)\int_{-d/2}^{d/2} V_z(x')\,H_0^{(1)}(k_0 R)\,dx', \tag{4}$$

$$E_x^{sc} = (Z_0/4k_0)\int_{-d/2}^{d/2} W_x(x')\,\frac{\partial^2}{\partial y^2}H_0^{(1)}(kR)\,dx', \tag{5}$$

where $R=\sqrt{(x-x')^2+y^2}$ and due to the decoupling we can say that $V_z$ produces no $E_x$ field and $W_x$ produces no $H_z$ field on the surface of the strip i.e. on $y$ = 0 plane. Then by imposing the boundary conditions given in (1a) and (1b), the following SIEs can be derived:

$$\kappa\int_{-1}^{1} V_z(t')\,H_o^{(1)}(\kappa|t-t'|)\,dt' + 4Q_{GDG}\,V_z(t) = 4Z_0\, e^{-i\kappa t\cos(\varphi_{in})} \tag{6}$$

$$\int_{-1}^{1} \tilde{W}_x(t')\sqrt{1-(t')^2}\,\frac{H_1^{(1)}\left(\kappa|t-t'|\right)}{|t-t'|}dt' + 4R_{GDG}\,\tilde{W}_x(t)\sqrt{1-t^2} = 8\sin(\varphi_{in})e^{-i\kappa t\cos(\varphi_{in})} \tag{7}$$

In the derivation of the above equations, we used $t = 2x/d$ parameterization and $\kappa = k_0 d/2$. Furthermore, due to the end point condition on the $W_x$ current density, we can decompose this function as $W_x(t) = \tilde{W}_x(t)\sqrt{1-t^2}$ .

These two SIEs (equations (6) and (7)) are solved by using the Nystrom methods. The first one that is the equation (6) is discretized by using the Gauss-Legendre quadrature rule and it is efficient in the solution of the logarithmic type singularity. This rule with the $n_v$ order uses the nodes which are nulls of the Legendre polynomials $P_{n_v}(\tau_j)=0, j=1,2,...,n_v$ . The second equation is transformed into a matrix equation by using the Gauss-Chebyshev quadrature rules. This rule with the $n_W$ order uses the Chebyshev nulls of $t_j=\cos(\pi j/(n_W+1))$, $j$ = 1,2, …,$n_W$. In these SIEs the singular and hyper singular kernels can be presented as the following expressions:

$$H_0^{(1)}\left(k|t-t'|\right)=\left(\frac{2i}{\pi}\right)\ln|t-t'|+M\left(t,t'\right) \tag{8}$$

$$\frac{H_1^{(1)}\left(k|t-t'|\right)}{|t-t'|}=\frac{ik\ln|t-t'|}{\pi}-\frac{2i}{\pi k|t-t'|^2}+N(t,t'), \tag{9}$$

where $N(t,t')$ and $M(t,t')$ are regular functions. This type of the Nystrom method depends on the accurate evaluation of the discrete singular integrals. There is one more alternative of the same technique and it is called numerical locally correction method. However the presented one used in this study is very suitable especially in the computation of the scattering from the basic geometries like a strip. The details of the technique can be found in [14]. Even though this is not a regularization type solution, the results show the high-rate convergence behavior. This means that the accuracy of the approximate numerical solution is improved when truncating the system with progressively larger sizes. The obtained data can be used as a benchmark for the comparisons of the other techniques.

## III. Scattering and Absorption Characteristics

The total scattered magnetic and electric fields in the far zone from the both surface current densities take the form $H_z^{sc} = \sqrt{2/i\pi kr}\,e^{ikr}\,\phi(\varphi)$ and $E_\varphi^{sc} = \eta_0 H_z^{sc}$, respectively.

The total scattered field pattern can be written as follows:

$$\phi(\varphi)=-\frac{\kappa}{4Z_0}\int_{-1}^{1}V_z(t')e^{-i\kappa t'\cos(\varphi)}dt' + \frac{\kappa}{8}\sin(\varphi)\int_{-1}^{1}\tilde{W}(t')\sqrt{1-(t')^2}\,e^{-i\kappa t'\cos(\varphi)}dt' \tag{10}$$

Then the total scattering cross section (TSCS) can be obtained by using the following equation:

$$\sigma_{tsc}=\frac{2}{\pi k}\int_0^{2\pi}|\phi(\varphi)|^2\,d\varphi \tag{11}$$

Another characteristic is the absorption cross section (ACS). It can be obtained from the optical theorem valid for both near and far zone fields of the strip [17]. This consideration leads to ACS expressed via the far-filed characteristics only,

$$\sigma_{abs}=-\sigma_{tsc}-\frac{4}{k}\mathrm{Re}\,\phi(\pi+\varphi_{in}) \tag{12}$$

## IV. Numerical Results

The numerical accuracy and convergence of the given formulation have been verified by using the relative error plots for the current densities and the total scattering cross section. The relative error for the $V_z$ current density can be written as the $error1=|\eta_V(n_v)-\eta_V(n_v=600)|/|\eta_V(n_v=600)|$ and the relative error for the $W_x$ current density can be given as the $error2=|\eta_W(n_W)-\eta_W(n_W=600)|/|\eta_W(n_W=600)|$. Furthermore then $\eta_V=\max|V_z(t_i)|$ and $\eta_W=\left[\int_{-1}^{1}|W_x(t)|^2\sqrt{1-t^2}\,dt\right]^{1/2}$

Similarly the relative error in the total scattering cross section can be measured by the following function $error3=|\sigma_{tsc}(n)-\sigma_{tsc}(n=600)|/|\sigma_{tsc}(n=600)|$ where $n_V$ is taken as equal to $n_W$ that is $n = n_V = n_W$. In all these relative error computations, the parameters are compared to results obtained with sufficiently large $n$ value ($n$ = 600 is taken).

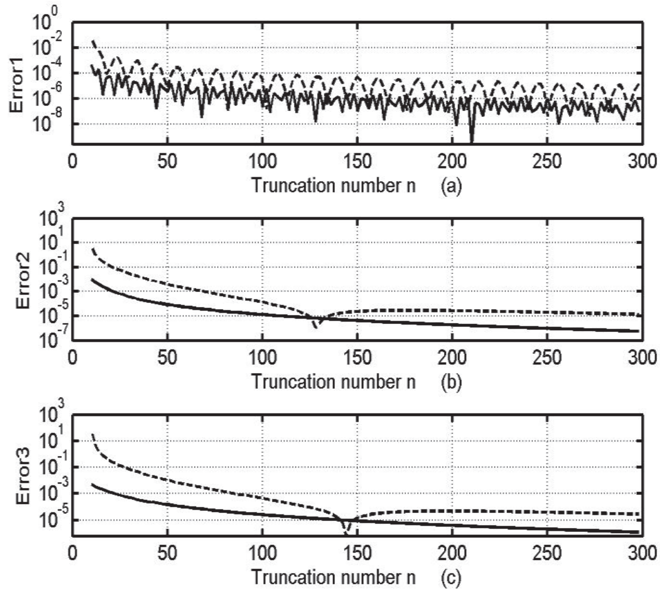


Fig. 2: The relative error plots for the current densities and the total scattering cross section: solid lines for the frequency of 5 THz and dashed lines for the frequency of 15 THz. The problem parameters are $\varepsilon_r$ = 20+0.1$i$, $\varphi_{in}$ = 90º, $h$ = $d$/200, $d$ = 100 μm, $\mu_c$ =0.3 eV, $T$ = 300K, $\tau$ = 1ps.

In Fig. 2, the relative error functions computed as explained above are plotted. As expected, the level of the relative errors for all considered parameters is quite good for the 5 THz and even for the 15 THz cases and goes down with larger values of $n$. This validates the convergence of our codes and hence we can search further results for the scattering and absorptions of THz waves by a composite graphene-dielectric-graphene strip

In Fig. 3, both ACS and TSCS are plotted as a function of the frequency and the oscillations on the plots due to the SP resonances are observed. The effect of the SP resonances is present in the lower frequency region. If the frequency gets larger than the graphene effect reduces and all curves approaches to the thin dielectric strip curve obtained in [15]. Note that if the frequency is getting higher, then as a result of this increase, the graphene layer becomes more and more transparent because its surface impedance $Z$ grows up and exceeds the free-space impedance value. Therefore the effect of the graphene disappears and only the effect of the thin dielectric strip remains at sufficiently high frequencies. We also observe that the increase in the chemical potential $\mu_c$ shifts the SP resonance region to the right and the resonance peaks are seen more easily. For example in ACS plot the number of the oscillation peaks increases when $\mu_c$ getting higher. It can also be expected that the comments about the SP resonances of single graphene strip is valid for this case, but these will be examined in a more detailed study.

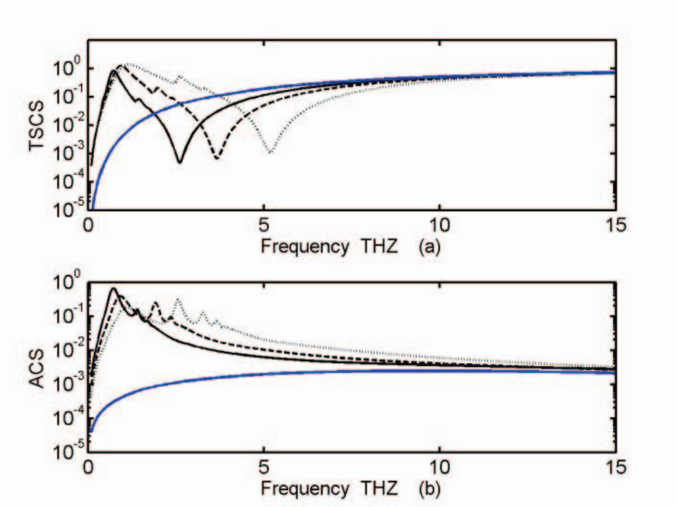


Fig. 3: Normalized total scattering and the absorbed cross sections variation with the frequency. These cross sections are normalized by the '2d' parameter in this figure. Solid blue line: no graphene case (only thin dielectric layer), solid line: $\mu_c$ = 0.1 eV, dashed line: $\mu_c$ = 0.2 eV, dotted line: $\mu_c$ = 0.4 eV. The problem parameters are $\varepsilon_r = 20 + 0.1i$, $\varphi_{in} = 90^o$, $h = d/200$, $d$ = 100 μm, $T$ = 300K, $\tau$ = 1 ps.

## V. CONCLUSIONS

A 2-D flat thin dielectric strip covered from both sides with graphene layers, placed in the free space, and illuminated by an H-polarized plane wave has been analyzed using SIEs and Nystrom technique. In this polarization case, for a single thin dielectric strip the TSCS and ACS curves show almost smooth nature, in the sense that no resonance oscillations can be seen. However if the same dielectric strip is covered with graphene, the SP resonance effect is clearly observed. Still the SP resonances due to the graphene and the other smooth variations of the thin dielectric strip are separated from each other in the frequency range. The former is seen at the lower frequency region and at the higher frequencies it is seen that almost no graphene effect. This study can also be expanded to the E-polarization case for the sake of the completeness.

## REFERENCES

[1] K. R. Jha and G. Singh, "Terahertz planar antennas for future wireless communication: A technical review," *Infrared Phys. Technol*., vol. 60, pp. 71–80, 2013.

[2] A. I. Nosich, "Method of analytical regularization in computational photonics," *Radio Sci*., vol. 51, no 8, pp. 1421-1430, 2016.

[3] R. Orta, P. Savi, and R. Tascone, "The effect of finite conductivity on frequency selective surface behavior," *Electromagnetics*, vol. 10, no 2, pp. 213–227, 1990.

[4] A. I. Nosich, Y. Okuno, and T. Shiraishi, "Scattering and absorption of E and H-polarized plane waves by a circularly curved resistive strip," *Radio Science*, vol. 31, no 6, pp. 1733-1742, 1996.

[5] E. Bleszynski, M. Bleszynski and T. Jaroszewicz, "Surface-integral equations for electromagnetic scattering from impenetrable and penetrable sheets," *IEEE Trans. Antennas Propagat. Mag*. vol. 36, no. 6, pp. 14-25 1993.

[6] A.Karlsson, "Approximate boundary conditions for thin structures," *IEEE Trans. Antennas Propag*., vol. 57, no. 1, pp. 144–148, 2009.

[7] M. V. Balaban, "Modeling of stratified graphene-dielectric structures using the generalized boundary conditions: THz wave scattering by a thin sandwiched disk," *Proc. Int. Conf. Electronics Nanotechnology (ELNANO-2015)*, Kiev, 2015, pp. 207-210.

[8] A. I. Nosich, "Method of analytical regularization in wave-scattering and eigenvalue problems: Foundations and review of solutions," *IEEE Trans. Antennas Propagat. Mag*. vol. 42, no.3, pp. 34-49, 1999.

[9] T. Oguzer, A. I. Nosich, and A. Altintas, "Analysis of arbitrary conic section profile cylindrical reflector antenna, H-polarization case," *IEEE Trans. Antennas Propagat*., vol. 52, no 11, pp. 3156-3162, 2004.

[10] T. Oğuzer, A. Altintas, and A. I. Nosich, "Analysis of the elliptic-profile cylindrical reflector with a non-uniform resistivity using the complex source and dual-series approach: H-polarization case," *Opt. Quant. Electron*., vol. 45, no 8, pp. 797-812, 2013.

[11] T. L. Zinenko and A. I. Nosich, "Plane wave scattering and absorption by flat gratings of impedance strips," *IEEE Trans. Antennas Propagat*., vol. 54, no 7, pp. 2088-2095, 2006.

[12] T. L. Zinenko, "Scattering and absorption of terahertz waves by a free-standing infinite grating of graphene strips: analytical regularization analysis," *J. Optics*, vol. 17, no 5, pp. 055604/8, 2015.

[13] T. L. Zinenko, A. Matsushima, and A. I. Nosich, "Surface-plasmon, grating-mode and slab-mode resonances in THz wave scattering by a graphene strip grating embedded into a dielectric slab," *IEEE J. Sel. Top. Quant. Electron*., vol. 23, no 4, art. no 4601809, 2017.

[14] M. V. Balaban, E. I. Smotrova, O. V. Shapoval, V. S. Bulygin and A. I. Nosich, "Nystrom-type techniques for solving electromagnetics integral equations with smooth and singular kernels" *Int. J. Num. Modelling: Electronic Networks, Devices Fields*, vol. 25, no 5, pp. 490-511 2012.

[15] O. V. Shapoval, R. Sauleau and A. I. Nosich, "Scattering and absorption of waves by flat material strips analyzed using generalized boundary conditions and Nystrom-type algorithm," *IEEE Trans. Antennas Propagat*., vol. 59, no. 9, pp. 3339-3346, 2011.

[16] M. V. Balaban, O. V. Shapoval, and A. I. Nosich, "THz wave scattering by a graphene strip and a disk in the free space: integral equation analysis and surface plasmon resonances," *J. Optics*, vol. 15, no 11, pp. 114007/9, 2013.

[17] O. V. Shapoval, J. S. Gomez-Diaz, J. Perruisseau-Carrier, J. R. Mosig, and A. I. Nosich, "Integral equation analysis of plane wave scattering by coplanar graphene-strip gratings in the THz range," *IEEE Trans. Terahertz Science Technol*., vol. 3, no 5, pp. 666-673, 2013.

[18] O. V. Shapoval and A. I. Nosich, "Bulk refractive-index sensitivities of the THz-range plasmon resonances on a micro-size graphene strip," *J. Phys. D: Appl. Phys*., vol. 49, no 5, pp. 055105/8, 2016.

[19] G. W. Hanson, "Dyadic Green's functions and guided surface waves for a surface conductivity model of graphene," *J. Appl. Phys*., vol 103, no. 6, pp. 064302/8, 2008.

[20] D. Colton and R. Kress, *Integral Equation Method in Scattering Theory*, Wiley Publ., 1983.

[21] M. Born and E. Wolf, *Principles of Optics*, Pergamon Press, 1980.